

AD-A099 452

NAVAL RESEARCH LAB WASHINGTON DC

PROGRESS AND TRENDS IN X-RAY LASER RESEARCH USING HYDROGENIC F/G 20/1

MAY 81 R C ELTON

NRL-NR-4525

UNCLASSIFIED

AM

100

100

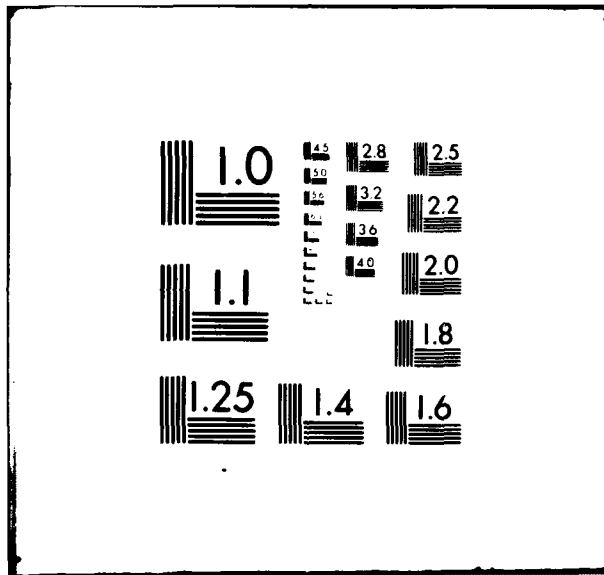
END

DATE

ENTERED

6 81

DTIC



AD A099452

SECURITY CLASSIFICATION OF THIS PAGE (When Data Entered)

(14) NRL-MR-4525

REPORT DOCUMENTATION PAGE		READ INSTRUCTIONS BEFORE COMPLETING FORM
1. REPORT NUMBER NRL Memorandum Report, 4525	2. GOVT ACCESSION NO. AD-A099452	3. RECIPIENT'S CATALOG NUMBER
4. TITLE (and Subtitle) PROGRESS AND TRENDS IN X-RAY LASER RESEARCH USING HYDROGENIC IONS		5. TYPE OF REPORT & PERIOD COVERED Interim report on a continuing NRL problem.
6. PERFORMING ORG. REPORT NUMBER		7. AUTHOR(s) R. C. Elton
8. CONTRACT OR GRANT NUMBER(s)		9. PERFORMING ORGANIZATION NAME AND ADDRESS Naval Research Laboratory Washington, DC 20375
10. PROGRAM ELEMENT, PROJECT, TASK AREA & WORK UNIT NUMBERS 65-1152-0-1, 65-1153-0-1		11. CONTROLLING OFFICE NAME AND ADDRESS
12. REPORT DATE May 27, 1981		13. NUMBER OF PAGES 14
14. MONITORING AGENCY NAME & ADDRESS (if different from Controlling Office)		15. SECURITY CLASS. (of this report) UNCLASSIFIED
16. DISTRIBUTION STATEMENT (of this Report) Approved for public release; distribution unlimited.		17. DECLASSIFICATION/DOWNGRADING SCHEDULE
18. DISTRIBUTION STATEMENT (of the abstract entered in Block 20, if different from Report)		
19. SUPPLEMENTARY NOTES		
20. KEY WORDS (Continue on reverse side if necessary and identify by block number) X-ray lasers Recombination Charge transfer Plasma ions		
21. ABSTRACT (Continue on reverse side if necessary and identify by block number) → Progress in the research devoted to developing x-ray lasers will be reviewed as it pertains to one-electron hydrogenic ions created and pumped to inversion in high- density laser-produced plasmas. A simple analysis defines a useful parameter space. Measured gain coefficients for C^{5+} are in good agreement with modeling for electron- capture pumping. Photon pumping is identified for possible circumvention of radiative-trapping limitations in larger volumes. Preliminary data on aluminum appear (Continues)		

DTIC
ELECTIC
MAY 27 1981

DD FORM 1 JAN 73 1473

EDITION OF 1 NOV 65 IS OBSOLETE
S/N 0102-014-6601

SECURITY CLASSIFICATION OF THIS PAGE (When Data Entered)

251950

20. ABSTRACT (Continued)

promising for shorter wavelength extrapolation. The advantage of efficient x-ray cavities is apparent. Extension of the illustrative analysis provides directions for future quantitative measurements leading to large scale gain experiments.

CONTENTS

INTRODUCTION	1
ANALYSES	1
EXPERIMENTAL COMPARISONS	4
SUMMARY	6
ACKNOWLEDGMENT	6
REFERENCES	6

Accession For	
NTIS GRA&I	<input checked="checked" type="checkbox"/>
DTIC TAB	<input type="checkbox"/>
Unannounced	<input type="checkbox"/>
Justification	
By _____	
Distribution/	
Availability Codes	
Dist	Avail and or Special
A	

PROGRESS AND TRENDS IN X-RAY LASER RESEARCH USING HYDROGENIC IONS*

Introduction

Research towards achieving an x-ray laser has been progressing steadily in a rather modest worldwide effort since the early 1970's. A number of review articles have been published at various times on both research^{1,2} and applications^{3,4}; no attempt will be made here to review the field again. Rather, the purpose here is to gather some meaningful quantitative spectroscopic data on gain coefficients and population densities as well as plasma densities and temperatures, and to show that these data compare favorably with a rather simple analysis based on established physical principles. Such an analysis provides a suitable parameter space that encompasses several experiments with both carbon and aluminum ions, and indicates some directions in which future research could provide valuable data needed for defining high-gain test experiments involving large pump lasers.

Analyses

The following simple analyses are not intended to replace the elegant computer programs that have been developed for modeling atomic and plasma dynamic processes in laser-produced plasmas. Rather, the intent is to use a few basic physical principles to estimate the gain and the associated plasma parameters for comparison with some quantitative data. In essence, the end justifies the means in that reasonably good agreement is found, so that the physical intuition provided from the basic principles invoked permits both the evaluation of current experiments and the formation of some projections for future experiments with confidence, hopefully to be supported by extended numerical computations.

Gain relations

General. The challenge of achieving gain $I/I_0 = \exp(GL)$ over a length L at increasing photon energy derives directly from a (positive) gain coefficient G , which is related to the cross sections for induced emission and resonance absorption and the upper and lower state population densities N_u , N_l

$$G = N_u \sigma_{\text{ind}} - N_l \sigma_{\text{abs}} = \frac{\pi r_0^2 c f}{\Delta \nu} \cdot \frac{g_l}{g_u} \cdot \left[N_u - N_l \left(\frac{g_u}{g_l} \right) \right], \quad (1)$$

where r_0 is the classical electron radius, f is the absorption oscillator strength, g_u , g_l are the upper and lower state statistical weights, and $\Delta \nu$ is the line width in frequency units. For a Doppler-broadened line at a mean thermal velocity \bar{v}_D , $\Delta \nu_D / \nu = \bar{v}_D / c$, or

$$\Delta \nu_D = 2\nu \left(\frac{2kT}{Mc^2} \ln 2 \right)^{1/2}, \quad (2)$$

where the radiating particle mass and temperature are given by M and T , respectively. The Doppler-gain coefficient then becomes (with $\nu = c/\lambda$ and a factor of $\sqrt{\ln 2}$ included for Gaussian line shapes):

*Some of this material was presented as part of an invited talk at the 11th Winter Colloquium on Quantum Electronics, Snowbird, Utah, January 14-16, 1981.

To be published in Proceedings of the SPIE Technical Symposium East '81, in Washington, DC April 20-24, 1981, paper 279-10.

Manuscript submitted March 30, 1981.

$$G_D = \frac{\pi^2 r_0 c \lambda f(g_u/g_l)}{2} \left(\frac{M}{2\pi kT} \right)^{1/2} N_u \left[1 - \frac{N_l}{N_u} \frac{g_u}{g_l} \right]. \quad (3)$$

This shows an explicit linear dependency on wavelength and the importance of the upper state density in achieving significant gain, once the bracketed factor becomes positive to assure a population inversion, rather than resonance absorption. Implicit here however is the wavelength dependence of the pumping process, since in equilibrium

$$N_u \approx \frac{N_0 P}{A}, \quad (4)$$

where P is the pumping rate out of an initial ion state of density N_0 and A is the total depopulation rate.

Hydrogenic ions. The above is general. By next specifying that the ions be hydrogenic, i.e., stripped of all but one electron, the gain analysis continues relatively straightforward, because of the simplicity of the one-electron structure. Also, potential losses associated with processes such as photoionization and autoionization involving outer electrons are avoided. With $M = 2$, $A = Z^{-4}$ for radiative depopulation, $\lambda = Z^{-2}$, and $T = Z^2$, the gain coefficient then scales as $P N_0 Z^{-13/2}$, so that a strong scaling of $P N_0$ with Z is required for the favorable extrapolation of high gain to increased Z and shorter wavelengths along the hydrogenic isoelectronic sequence.

Recombination pumping. Pumping of ionic population inversions is achieved the most naturally in plasmas using the free electrons available in quasi-neutrality. The capture of free electrons into high-lying states (collisional recombination) followed by cascade, and the collisional excitation or ionization of bound electrons into excited states are two examples. These can be analyzed fairly reliably and form an inversion basis, which then can be augmented by, for examples, charge transfer of bound electrons from neutral atoms^{6,7} and photon (flashlamp) pumping⁸, when such pump energy and the proper resonant matches are available for efficient pumping. We will continue here with the analysis based upon recombination onto fully-stripped ions, which has been extensively analyzed since its first suggestion⁹ in 1965. In such a quasi-neutral fully-ionized plasma, the free electrons are abundant in proportion $n \approx N_e/N_0 = Z$ and a quasi-cw inversion is obtained between excited states in a cascade when the lower states are depopulated to the ground state more rapidly than are the upper states. The desired recombination rate product $N_0 \cdot P_r$ may be approximated by¹⁰

$$N_0 P_r \approx \frac{10^{-31} N_e^2 N_0 (n')^6}{Z^6} \left(\frac{Z^2 R_y}{kT_e} \right)^2 \exp \left[\frac{Z^2 R_y}{(n' + 1)^2 kT_e} \right] \text{ sec}^{-1} \text{ cm}^{-3}, \quad (5)$$

where the Rydberg, $R_y = 13.56 \text{ eV}$, represents the hydrogen ionization potential, $N_e = Z^7$ (see below) is the free electron density, and n' is the so-called collision-limit quantum number^{10,11}, i.e., the energy level at which electron collisional excitation from that level equals the radiative decay to lower levels. Notice the increased pumping at reduced electron temperatures, indicated here by the T_e^{-2} dependence. From Eq. (5), assuming $N_0 = N_e/Z = Z^6$, the scalings with Z become:

$$N_0 P_r = Z^{14} \quad (6)$$

and

$$G_r = Z^{7.5}, \quad (7)$$

which are very favorable, providing all other conditions scale within reason for experiments. Actual values for this gain will be given later.

Charge transfer pumping. Closely akin to free-electron capture is bound-electron capture or charge transfer of an electron from a (neutral) atom to a stripped ion, resulting in preferential population of a specific excited level(s) in a hydrogenic ion. The cross section for the resonance charge transfer (rct) process is approximated by

$$\sigma_{rct} \approx \pi a_0^2 Z^2 \quad (8)$$

(where the Z^2 scaling is probably optimal), and a rate of

$$P_{rct} \approx N_A \langle \sigma v \rangle \approx N_A \pi a_0^2 Z^2 \bar{v}. \quad (9)$$

Here N_A is the neutral density, and a_0 is the Bohr radius. In vacuum a carbon plasma at $T_e = 200$ eV expands at a speed of $\sim 10^7$ cm/sec which scales approximately as $(T_e/M)^{1/2}$. Therefore

$$N_0 P_{\text{ret}} \approx N_0 N_A a_0^2 Z^2 (10^7) \left(\frac{kT_e}{200} \cdot \frac{6}{Z} \right)^{1/2} \text{ sec}^{-1} \text{ cm}^{-3}, \quad (10)$$

which scales with Z as

$$N_0 P_{\text{ret}} = Z^{14.5}, \quad (11)$$

so that

$$G_{\text{ret}} = Z^8, \quad (12)$$

assuming that the neutral atoms are created by direct sputtering by the ions, i.e., $N_A = N_e/Z = Z^6$ also. Thus, the scaling is similar to that for capture of free electrons by the ions.

Collision limit on inversion

Population inversions formed by cascade can only be expected to exist for electron densities low enough that collisional depopulation from the upper to the lower laser levels does not dominate over radiative decay. This upper limit on electron density in the plasma is found by equating the electron-collisional deexcitation rate¹⁰ to the corresponding radiative-transition probability. The Z -scaling for the equation is N_e/Z^7 and $T_e/Z^2 \text{ Ry}$, where $Z^2 \text{ Ry}$ is the hydrogenic-ion ionization potential. Such limiting lines are plotted in Fig. 1 for four possible laser transitions: 3-2, 4-2, 4-3, and 5-3. Above each of these lines population inversion becomes zero or negative (absorption), and also Stark broadening enters which would further reduce the gain. Such density-limiting lines are reproduced in the other figures as well.

In Fig. 2 values of n' calculated for high $n+1$ to n transitions are indicated on the right ordinate for comparison. It appears that $n' \approx (2n+1)/2$ might be a reasonably consistent approximation at high temperatures ($T_e/Z^2 \text{ Ry} > 0.5$), but cannot be used directly for low-lying levels and at low temperatures since the n' formulation^{10,11} is based on collisional excitation which includes an exponential low energy cutoff. It is instead collisional deexcitation¹⁰ that limits the inversion, for which a new collision-limiting quantum number $n'' \approx n' (g_l/g_u) \exp(\Delta E/kT)$ is defined and finally becomes

$$n'' \approx 126 \left(\frac{N_e}{Z^7} \right)^{-2/17} \left(\frac{kT}{Z^2 \text{ Ry}} \right)^{1/17}, \quad (13)$$

which will be recognized as the expression for n' without the exponential factor. The statistical weight ratio serves to counteract the high quantum state approximation in n' so that n'' here is appropriate for potential low-lying laser transitions. This resembles the "thermal limit" of Wilson¹² which included deexcitation with the exponential factors removed, but for a different reason, namely in the high- n and high- T limits. The n' (or n'') approximation remains a first-order approximation to the collision limit on inversion, at best.

Pump power requirements

There is a practical reason for desiring to operate near the collision limits shown in the figures. The gain depends directly on the upper state density N_u as shown in Eq. (3), as does the pump power density $W \approx N_u h\nu$ which is required to overcome losses. A large value of W is also required to obtain sufficient plasma temperature to achieve complete ionization (Fig. 1, discussed below). For $G=5 \text{ cm}^{-1}$ and a 3-2 transition, W at various wavelengths λ is given¹ in Table 1, using N_u from Eq. (3). Note that for C^{5+} at $\lambda = 18.2 \text{ nm}$ a plasma power density of 30 GW/cm^3 is required. Also note that wavelengths as short as 1 nm can be pumped with laser-fusion-sized focused Nd-glass lasers, for example.

Table 1. Pump Power Densities for $G=5 \text{ cm}^{-1}$

$\lambda =$	0.1	1	10	100	nm } Watts/cm ³ Plasma } Watt/cm ² Source*
$\log_{10} W =$	19	15	11	7	

*For 100 μm Depth, 1% coupling, laser-produced plasma.

Limited pumping power therefore necessitates small volumes including short lengths L , so that maximum gain products GL are achieved at the highest density possible. In other words, a reduced gain coefficient G at lower density cannot be compensated by a longer length L without increased pump power. This, plus the need for high plasma temperatures, is the reason that most x-ray laser research is performed on small plasmas created by focused high power (laser) beams.

Radiation trapping

Along with high density comes resonance trapping, particularly for the 2-1 Lyman- α transition. This trapping of resonance radiation can preferentially increase the lower state density and deplete the population inversion according to Eqs. (1) and (3). In the simplest case,

$$\frac{N_1 g_u}{N_u g_l} = \frac{A_{ul}}{A_{ll} g(\tau)} \cdot \left(\frac{n_u}{n_l} \right)^2, \quad (14)$$

where $g(\tau)$ is the so-called escape factor¹³, which is a function of the optical depth τ given by¹⁰

$$\tau = 5.5 \times 10^{-17} \lambda r N_1 D \left(\frac{u}{kT} \right)^{1/2} \quad (15)$$

for a laser diameter D , a hydrogenic ground state density N_1 (or $N^{(Z-1)+}$), an atomic mass number u , and with kT in eV. For a 3-2 transition the ratio in Eq. (14) reaches unity for $\tau \approx 3$, which determines the maximum permissible value of the product $N_1 D$. Obviously if complete stripping is maintained, N_1 will remain negligibly small; but that is unlikely as the temperature is lowered for increased pumping. With plasma quasi-neutrality it is more likely^{14,15} that $N_1 \approx N_e/10$. The maximum plasma diameter determined at the maximum electron density allowed by collisional equilibrium in Fig. 1 then scales as $Z^{-9/2}$ for all temperatures, and values are indicated in parentheses in Fig. 1 at the collision boundary. Recall once again that this is actually a ND limit and therefore D_{\max} will scale upward as N_e/Z is decreased.

Photon-assist pumping

It is obvious that the most severe limitations are placed on the $n=2$ transitions, again due to the strong 2-1 Lyman- α resonance line. Photon-assist pumping of $n=2$ electrons into specific higher- n states without perturbing the upper state populations would alleviate this lower state saturation considerably⁶. For example, Lyman- α radiation from a $Z/2$ ion would match at 2-4 excitation in ion Z and likewise $Z/3$ ion Lyman- α emission would match a 2-6 transition in ion Z . Intuitively, the lower transition rates at lower Z indicate the need for higher densities and temperatures in the pump source, so that the pump and the laser plasmas could not be congruent, and the emitter/absorber coupling becomes a crucial factor.

At the blackbody limit, the pump rate $P(2-4)$ compared to the depopulation rate $A(2-1)$ is given by⁸

$$\frac{P_{24}}{A_{21}} = \frac{1}{2} \left(\frac{g_4}{g_2} \right) \frac{A_{42}}{A_{21}} \left[\exp(h\nu/kT) - 1 \right]^{-1} \geq 1, \quad (16)$$

and must exceed unity for significance. This reduces to $h\nu/kT \leq 0.04$ where $h\nu(4-2) \approx Z^2 \text{ Ry}/5$, so that $kT \geq 5Z^2 \text{ Ry} \approx 70Z^2$ is required. At such a temperature there would not be a significant density of hydrogenic ions as pump sources. Higher- Z ions with coincident wavelengths or a filtered broadband flashlamp remain somewhat more promising possibilities.

Experimental Comparisons

Inversions along trajectories

Returning to Fig. 1, typical laser power densities W_L required to strip atoms of C, O and Al are indicated by vertical barriers. Such vertical divisions of the parameter space do not prohibit population densities, but rather define the zone of high ion density for high gain. The Log W scales are shown at N_e/Z values corresponding to a critical density $N_e = 10^{21} \text{ cm}^{-3}$ for 1 μm laser absorption; for Al, values for 2v and 4v frequency doubling and quadrupling are also indicated. Notice that all four transitions can be pumped near the maximum density in carbon with a 1 μm laser, but not the 4-2 transition in oxygen and only the 4-3 transition in Al without frequency multiplication into the ultraviolet region.

Of course, all can be pumped at densities below the collisional cutoff level at lower gain and increased pump demands, as discussed above.

Also shown in Fig. 1 are data points from Hull University¹⁶ (UH) [C(3-2)], Culham Laboratory¹⁷ (CU) [C(3-2, 4-2, 4-3)], Naval Research Laboratory^{6,7} (NR) [C(4-3)], and University of Rochester¹⁸ (UR) [Al(4-3) helium-like] with the closed points indicating where population inversion or gain measurements are reported, and open points where no inversion was observed. The numbers in brackets refer to distances from laser-heated targets. The 4-3 data are consistent with both the collisional deexcitation limit and radiative trapping for diameters $\sim 1/3$ to $1/2$ the distances indicated. The 3-2 and 4-2 data from Culham showing inversions only for $N_e/27$ less than 10^{12} cm⁻³ are also consistent with a plasma size approximately 30-times greater than permitted at 10^{14} cm⁻³, i.e., the $N_e D$ scaling behaves as expected (see Fig. 5). The 3-2 data from Hull University remain an enigma; although the size could be tolerable for radiative trapping limitations if the plasma produced from a thin fiber expands in a heated shell of thickness ~ 10 μ m, an electron density well above that expected to include collisional mixing will lead to a very small or even negative population inversion (see below).

Continuing in Fig. 2, extended trajectories originating in the critical density layer near the target are plotted for C and Al ions. Also, the density ratios $N_2^+/N_e \equiv \eta_2$ are shown where known^{4,15}. It is more important to maximize the density of stripped ions in the inversion region. This is best achieved by first completely stripping the atoms near the target and then following an isothermal trajectory towards lower densities, preferably maintaining a mean free path exceeding the final diameter anticipated for the gain medium. Mean free paths are plotted as (mm's) in Fig. 2. From this it is readily understood why η_6 is only $\sim 2 \times 10^{-6}$ (~ 10 mean free paths, i.e., $\sim e^{-10}$) when beginning at 10^{11} W/cm², and increases to ~ 0.05 at a higher initial pump flux level with complete ionization and a longer mean-free-path trajectory. Complete stripping in the Hull University experiments was anticipated¹⁶, also beginning at very high flux levels. For the University of Rochester experiments on Al, stripped-ion densities are not yet available; however complete stripping at the target is expected at 10^{15} W/cm² irradiation, and the mean free path is calculated to be greater than 10 mm.

Gain measurements

One reason that the ratios η_2 are available for carbon is that the density of stripped ions can be obtained from the absolute number density of hydrogenic ions in excited ($n=5, 6$ and 7 , e.g.) states lying near the continuum using Saha equilibrium calculations. These highly-excited state densities are conveniently obtained from the absolute emission of spectral lines in the near-ultraviolet region. Since the same excited states also radiate in resonance lines (e.g., $7-1, 6-1$), the branching ratio for radiative decay and the relative intensities in the resonance series provides a measurement of the upper laser state densities N_u in Eq. (3), from which the gain coefficient is obtained directly (with a known line width). The gains measured by this technique for carbon are shown as "f/meas" in Figs. 3-5. (The Hull University value in Fig. 5 was obtained from axial enhancement in a cylindrical plasma.) Again, these gain coefficients are measured directly in the experiments and do not depend on the assumption of any particular pumping model.

Gain modeled

Where the stripped ion density ratio η_2 is known along with the electron density and temperature, it is also possible to model the recombination gain from Eqs. (3) through (5). In Figs. 3-5 such a modeled gain is plotted at several magnitudes, for comparison with the direct measurements. In most cases a conservative inversion factor value $(1 - N_{e,g_1}/N_{e,g_2}) \approx 0.3$ is assumed. The agreement is generally good and in one case (Fig. 3, square point) some expected enhancement from resonance charge transfer pumping in a particular gaseous expansion experiment⁶ is indicated. For the University of Hull results, their assumption of $\eta_6 = 1/6$ (100% ionization) is used and a matching gain value of $G = 17$ cm⁻¹ is plotted for a best fit to a variable inversion factor giving $(1 - N_{e,g_1}/N_{e,g_2}) \approx 0.002$, much lower than the 0.3 value used at lower densities but apparently remaining positive for net gain. This low value would be consistent with the collisional regime in which that experiment appears to operate. No such modeling comparisons using the University of Rochester data (helium-like aluminum) have been done, because pertinent data are not yet available.

The gains modeled here do not restrict the parameter space available for population inversions and gain except for the particular recombination pumping mechanism assumed. For example, photon pumping or charge transfer pumping with adequate rates could occur throughout the space beyond the collision and ionization barriers, and again the modeling would depend on the specific external pumping source rather than the internal pumping by plasma electrons for recombination.

Summary

In summary, quantitative spectroscopy of hydrogenic (and helium-like^{6,7}) carbon ions is proving to be a valuable gauge for measuring directly the soft x-ray gain coefficient. The stripped-ion density and the inversion degree are also deduced as inputs for modeling. The gain coefficients measured so far for varying pump laser powers and transitions and locations relative to the irradiated target, as well as target configurations, are shown here to be in good agreement with a simple analytical model. The results are presented in such a way as to visualize progress, limitations, and prognoses. Preliminary data for helium-like aluminum, which requires more stringent parameters than carbon, look promising in this view, although similar quantitative spectroscopic data are more difficult to obtain. Increased target irradiation sustained for high temperatures during the plasma expansion beyond the collisional regime, followed by rapid cooling, would seem to be most desirable. Enhanced pumping by charge transfer and by photo-excitation, particularly in overcoming inversion depletion from radiative trapping, have been suggested as augmenting techniques in an otherwise optimized system. Clearly, more quantitative measurements of the sort described here, along with more expansive calculations are needed to project a large scale gain experiment at very short wavelengths. Supplementary to this is the need for the design of efficient ($\approx 50\%$ reflectivity) and durable cavities for the soft x-ray region.

Acknowledgement

This effort was supported by the Office of Naval Research and by the U. S. Department of Energy.

References

1. Waynant, R. W. and Elton, R. C., "Review of Short Wavelength Laser Research," Proc. IEEE, Vol. 64, pp. 1059-1092, 1976.
2. Elton, R. C., "Recent Advances in X-Ray Laser Research", in Advances in X-Ray Analysis, Vol. 21, C. S. Barrett and D. E. Leyden, eds., Plenum 1978.
3. Elton, R. C., "X-Ray Lasers", in Handbook of Laser Science and Technology, M. J. Weber, ed., CRC Press 1981.
4. Jorna, S., Ed., X-Ray Laser Applications Study, Report PD-LJ-77-159, Physical Dynamics, Inc., La Jolla, CA, 1977.
5. Nagel, D. J., "Potential Characteristics and Applications of X-Ray Lasers," Naval Research Laboratory Memorandum Report, 1981 (in press).
6. Dixon, R. H. and Elton, R. C., "Resonance Charge Transfer and Population Inversion Following C^{5+} and C^{6+} Interactions with Carbon Atoms in a Laser-Generated Plasma", Phys. Rev. Letters, Vol. 38, pp. 1072-1075, 1977; Dixon, R. H., Seely, J. F. and Elton, R. C., "Intensity Inversion in the Balmer Spectrum of C^{5+} ", Phys. Rev. Letters, Vol. 40, pp. 122-125, 1978.
7. Elton, R. C., Lee, T. N., Dixon, R. H., Hedden, J. D., and Seely, J. F., "Short Wavelength Population Inversions Associated with Charge Transfer in Laser-Produced Plasmas", in Laser Interaction and Related Plasma Phenomena, Vol. 5, M. J. Schwarz and H. Hora, eds., Plenum 1980.
8. Elton, R. C., Ed., "ARPA/NRL X-Ray Laser Program Final Technical Report", pp. 92-114, Naval Research Laboratory Memorandum Report no. 3482, 1977.
9. Gudzenko, L. I. and Shelepin, L. A., "Radiation Enhancement in a Recombining Plasma", Sov. Phys. JETP, Vol. 28, pp. 489-493, 1969.
10. Elton, R. C., "Atomic Processes", in Methods of Experimental Physics, Plasma Physics, Vol. 9A, Chapt. 4., H. R. Griem and R. H. Lovberg, eds., Academic 1970.
11. Griem, H. R., Plasma Spectroscopy, McGraw-Hill 1964, p. 160.
12. Wilson, R., "The Spectroscopy of Non-Thermal Plasmas", J. Quant. Spectros. & Rad. Transfer, Vol. 2, p. 482, 1962 (where Eq. (6) should show n_e^{-1}).
13. McWhirter, R. W. P., "Spectral Intensities", in Plasma Diagnostic Techniques, Chapt. 3, R. H. Huddleston and S. L. Leonard, eds., Academic 1965.
14. Irons, F. E. and Peacock, N. J., "A Spectroscopic Study of the Recombination of C^{6+} to C^{5+} in an Expanding Laser-Produced Plasma", J. Phys. B, Vol. 7, 1974.
15. Malvezzi, A. M., Garifo, L., Jannitti, E., Nicolosi, P., and Tondello, G., "XUV Spectroscopic Studies of a Carbon Laser Produced Plasma", J. Phys. B, Vol. 12, pp. 1437-1447, 1979.
16. Pert, G. J., "Extreme Ultraviolet Laser Action in Plasmas", Phil. Transactions Royal Society London, in press.
17. Irons, F. E. and Peacock, N. J., "Experimental Evidence for Population Inversion in C^{5+} in an Expanding Laser-Produced Plasma", J. Phys. B, Vol. 7, pp. 1109-1112, 1974.
18. Forsyth, J. M. and Contouris, Y., Private Communications 1979-80; also, Shadavutula, V. A. and Yaakobi, B., "Direct Observation of Population Inversion between Al^{+11} Levels in a Laser-Produced Plasma", Optics Comm., Vol. 24, pp. 331-335, 1978.

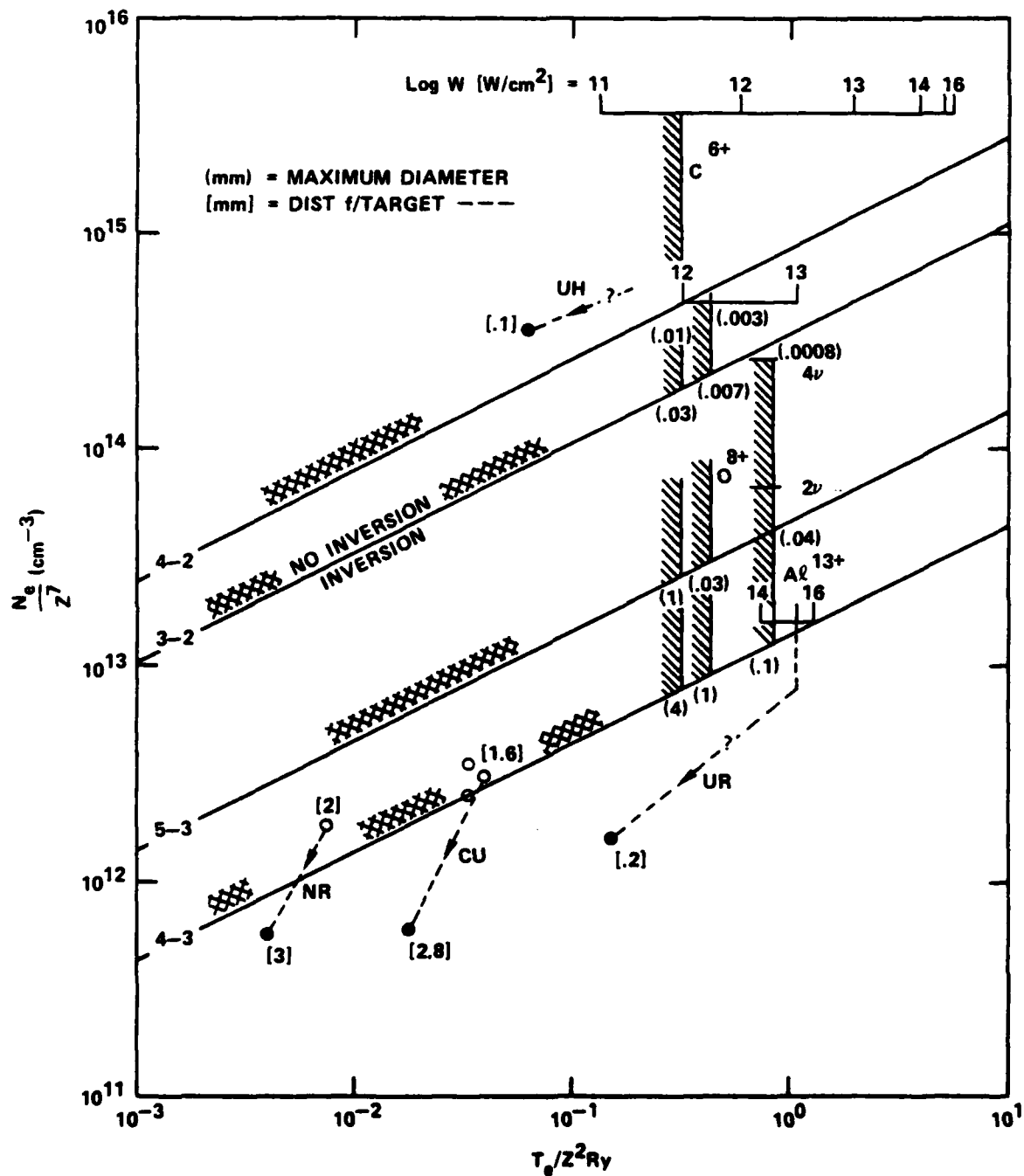


Fig. 1 -- Parameter space for achieving population inversions on several hydrogenic transitions

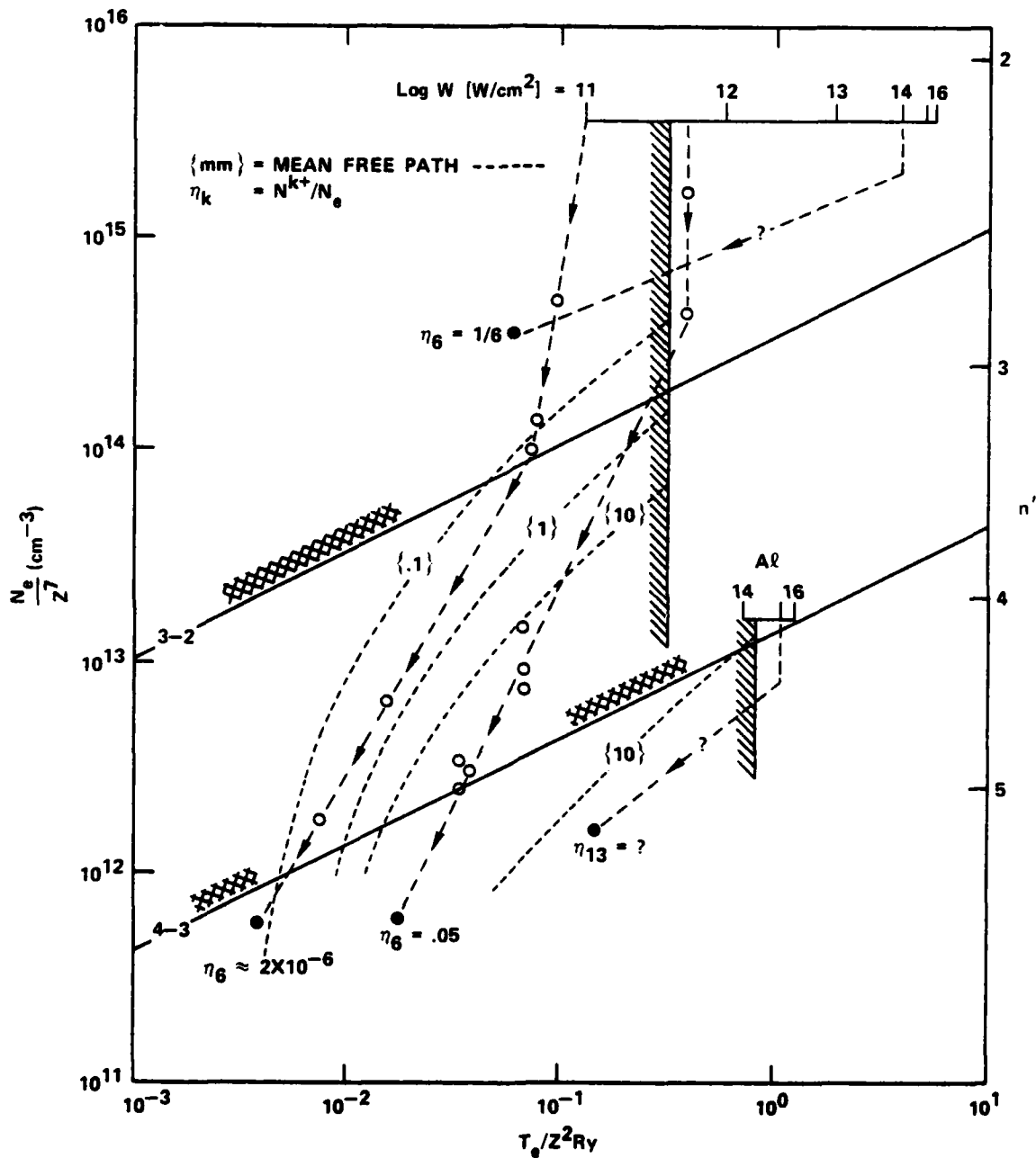


Fig. 2 — Trajectories (long dashes) in parameter space and mean free paths (short dashes)

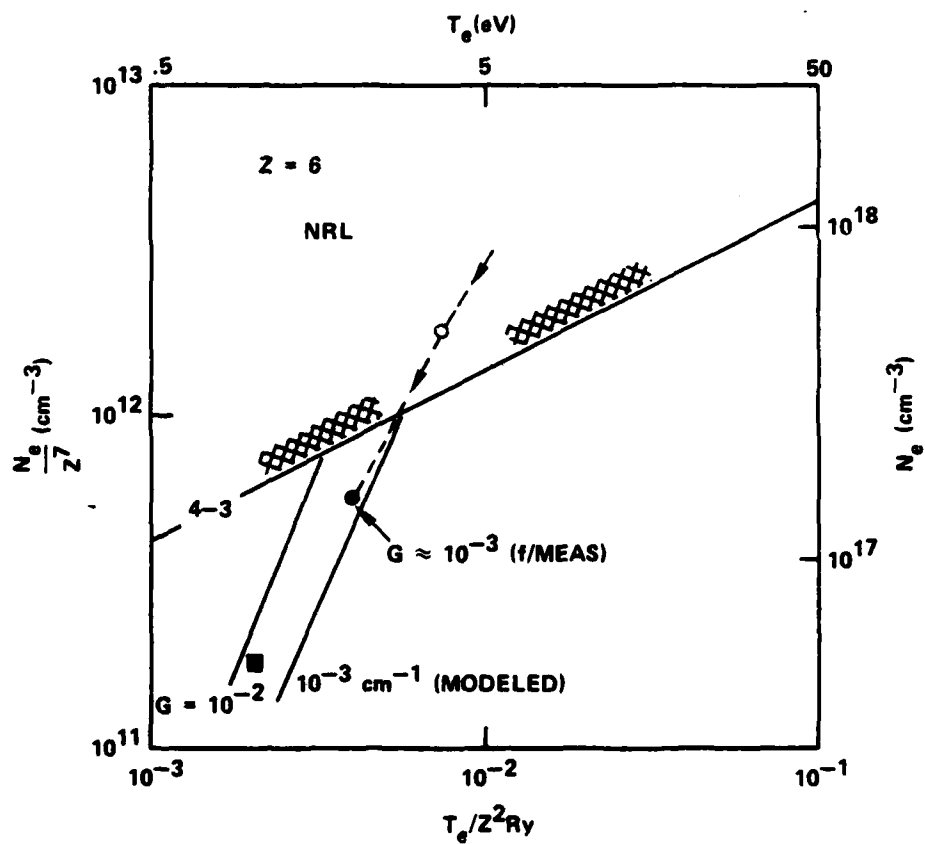


Fig. 3 - NRL gain with modeling

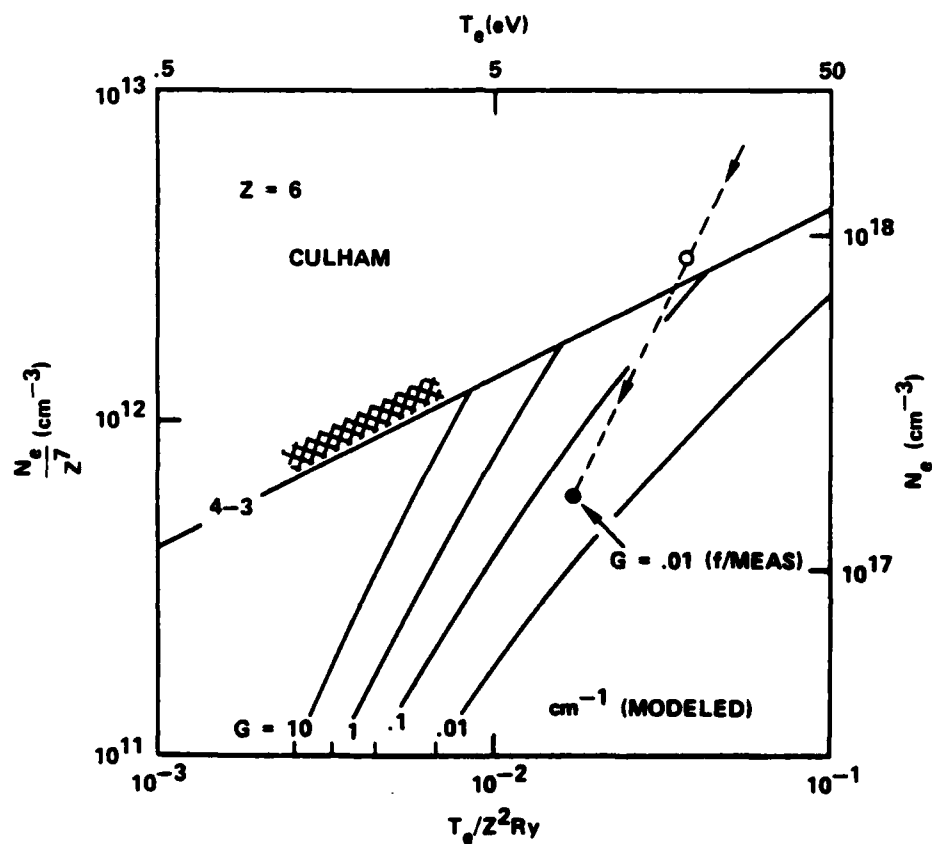


Fig. 4 - Culham gain with modeling

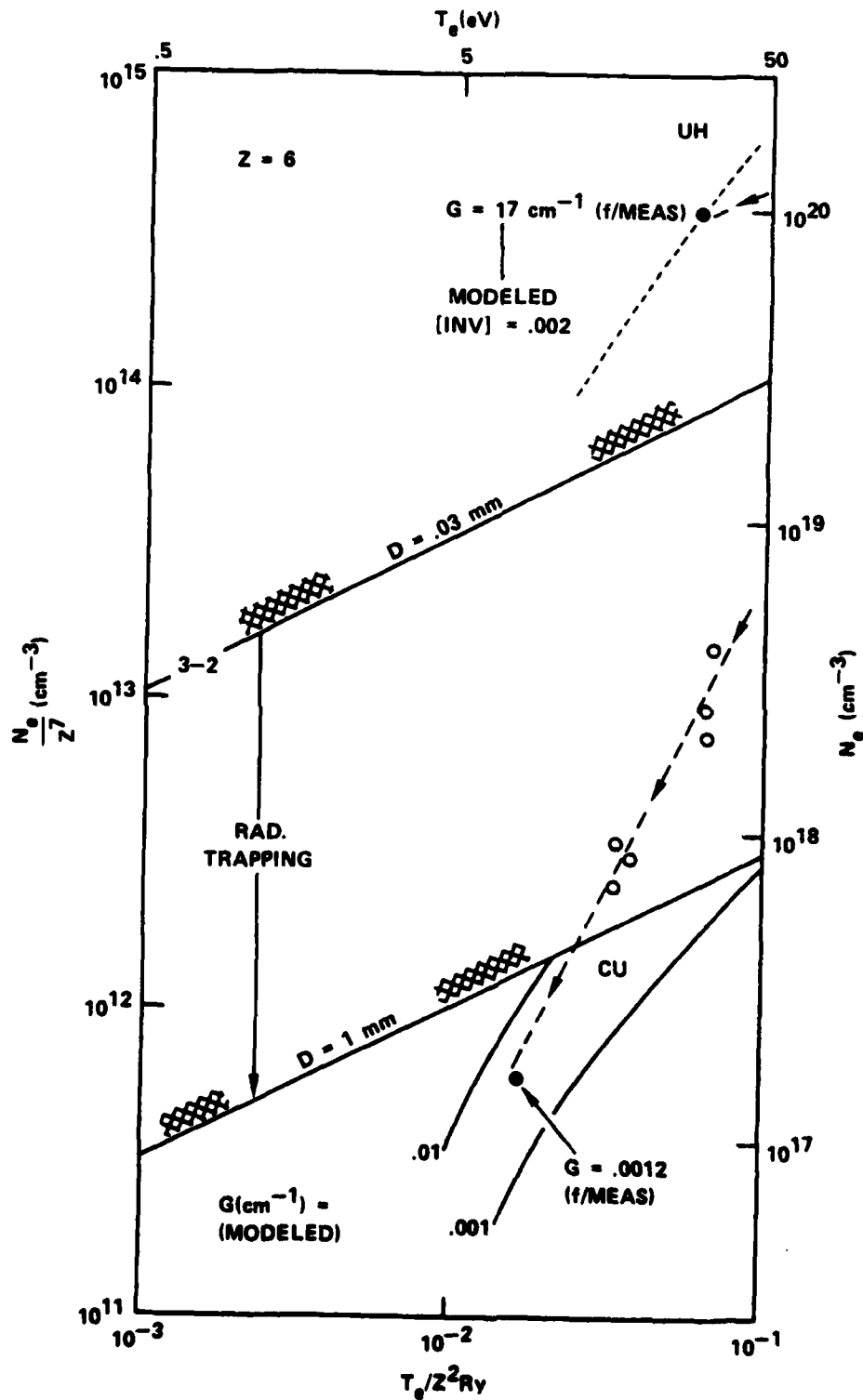


Fig. 5 - Culham and Hull gains with modeling for 3-2 transitions

**DAT
FILM
6 —**